

Latency Analysis of LEO Satellite Relay Communication: An Application of Conditional Contact Angle Distribution

Sixi Cheng and Xiang Ling

National Key Laboratory of Science and Technology on Communications

University of Electronic Science and Technology of China

Chengdu, China

Email: chengsixi@std.uestc.edu.cn, xiangling@uestc.edu.cn.

Abstract

This article investigates the transmission delay of a Low Earth Orbit (LEO) satellite communication system in a bent pipe structure. By employing a stochastic geometry framework, satellites are modeled as spherical binomial point processes (BPP). A suboptimal satellite relay selection strategy is proposed, which achieves optimal conditions through theoretical analysis and numerical exploration. We derive the distance distributions for the uplink and downlink links, and provide corresponding analytical expressions for the transmission delays.

Index Terms

Stochastic geometry, transmission delay, binomial point process, distance distribution, best relay selection.

I. INTRODUCTION

Ultra-dense LEO satellite network, because of its seamless global coverage characteristics, is likely to be utilized as a vital part of the future 6G system [1], [2]. Companies such as SpaceX,

Corresponding author: Xiang Ling, E-mail: xiangling@uestc.edu.cn. The condensed version of this article has been submitted to 2023 7th International Conference on Communication and Information Systems (ICCIS 2023) held in Chongqing, China.

Telesat, and OneWeb are accelerating the formation of a network of tens of thousands of LEO satellites [3]. In real time communication scenarios, satellites fundamentally play the role of a space relay or forwarder to connect two terrestrial stations [4], which can be considered as a terrestrial-satellite-terrestrial unit in long-distance transmission. This leads to a fact that the performance of a terrestrial-satellite-terrestrial unit is worthy to analyse.

Stochastic geometry, as an effective mathematical tool, plays a particularly important role in analyzing the performance of satellite networks [5], [6]. BPP model, which is relatively accurate for closed area networks with a fixed number of satellites, is used in [7] to analyse the coverage and rate of downlink. The user coverage probability for a scenario where satellite gateways (GWs) are deployed on the ground to act as a relay between the users and the LEO satellites is studied in [8]. Most of the authors of the focus on the downlink transmission performance of satellite-terrestrial, while the uplink transmission performance has not been extensively studied. [9] introduces contact angle distribution to analyze the influences of the number of satellites and the distance between the transmitter and receiver, which does not consider any channel fading [10]. As the Rician fading model is ubiquitous for the communication links between satellites and ground stations, we adopt shadowed-Rician (SR) fading for the channel between the satellite and the terrestrial station, which is pointed as most accurate channel model.

As for relay selection strategy, [11] proposes nearly optimal protocol in dual hop scenario. Therefore, based on the existing research, the contributions of this work are summarized as follows.

- We give a possible optimal relay selection strategy and explore under what conditions the relay selection strategy is approximately optimal.
- Under the certain relay selection strategy, we derive analytical expressions of the distance distribution of uplink and downlink and respectively give expressions for the cumulative distribution function of the signal-to-noise ratio (SNR), which take channel fading into consideration.
- Based on above, we derive analytical expressions of the total transmission delay. By simulation, we verify the accuracy of the total transmission delay and investigate the effect of power, number of satellites, and distance between transmitter and receiver on the total transmission delay.
- In the simulation, stochastic geometry is used to analyze the performance of satellite communications over multiple hops (or multiple links), which is not found in the existing

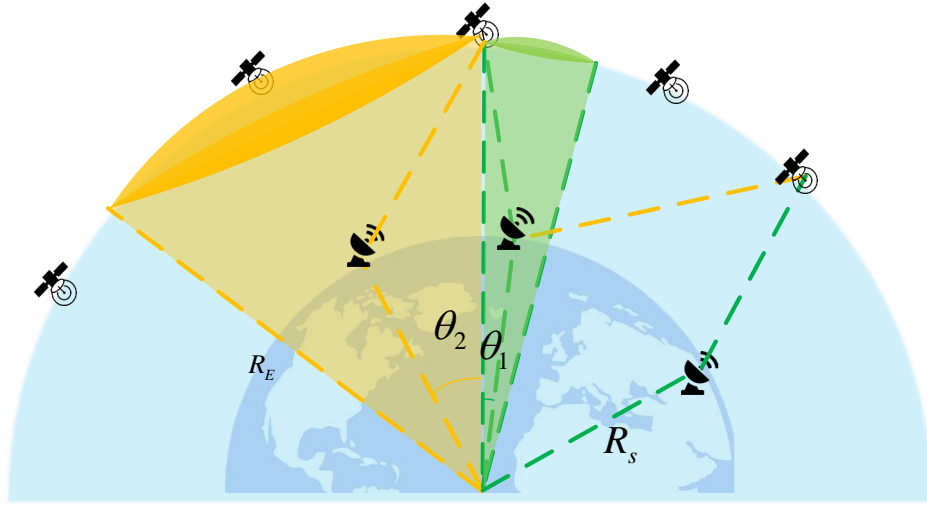


Fig. 1: System model.

papers.

II. SYSTEM MODEL

A. Network Topology

In this subsection, we build a terrestrial-satellite-terrestrial relay communication model. N_s satellites are distributed on a spherical surface with radius R_s and form a homogeneous BPP [12]. Since the BPP distribution remains the same after the rotation, the coordinates of the transmitter and receiver are set to at $(R_e, 0, 0)$ and $(R_e, \Theta, 0)$ for the convenience of calculation. The radius of the Earth is denoted as $R_e = 6371\text{km}$. Here, we consider that the terrestrial stations are fixed and the satellites obey the BPP distribution.

Although we analyze only one terrestrial-satellite-terrestrial unit here, in the simulation part we analyse the long-distance transmission with multi units. This implies that the unit model is also applicable to the long-distance transmission models.

B. Relay Selection

In fixed topology Amplify and Forward (AF) or Decode and Forward (DF) networks, the optimal relay selection criterion is the maximization of end-to-end SNR or the maximum SNR

of downlink. However, when the relay satellites form a BPP, analysis of this strategy is intractable. Therefore, we consider a slightly suboptimal but tractable selection strategy [13]: First, find a set of relays which can provide reliable communication for both the transmitter and receiver. Then, select the relay that has the strongest average received power in downlink. The reason for choosing the the strongest average received power in downlink is that: (i) In AF, the relay satellite amplifies the signal and also amplifies the noise. As a result, the downlink noise must be larger than the uplink. (ii) Considering that satellite energy is expensive, satellite transmission power is relatively low.

C. Channel Model

Many works have focused on deriving an accurate channel model for the communication links between satellites and ground stations, where it was shown that shadowed-Rician (SR) model proposed in [14] is the most accurate. So, we consider the SR model to calculate fade margins and analyze the performance of communication.

For the uplink, the received signal power $p_{(2)}^s$ at relay satellite is

$$p_{(2)}^s = p_{(1)}^s A_u \times W_t^2, \quad (1)$$

where A_u and W_t^2 respectively represent the propagation loss and the SR fading. The propagation loss can be calculated by:

$$A_u = \frac{G_{(1)}^e G_{(2)}^s \lambda_u^2}{(4\pi d_{\text{up}})^2 L_{(1)}^e L_{(2)}^s L_{\text{add}}}, \quad (2)$$

where $G_{(1)}^e$ and $G_{(2)}^s$ denote the transmitter and receiver antenna gain, λ_u denotes the carrier wavelength of uplink, d_{up} is the distance between the transmitter and the relay satellite, $L_{(1)}^e$ and $L_{(2)}^s$ denote the transmitter and receiver antenna feeder loss, L_{add} denotes the link additional loss, including atmospheric absorption loss, rain attenuation, etc.

The probability density function (PDF) of the SR fading power [14] W_t^2 is given as follows:

$$f_{W_t^2}(t) = \left(\frac{2b_0 m}{2b_0 m + \Omega} \right)^m \frac{1}{2b_0} \exp \left(-\frac{t}{2b_0} \right) \times \sum_{n=0}^{\infty} \frac{(m)_n}{(1)_n n!} \left(\frac{\Omega t}{2b_0(2b_0 m + \Omega)} \right)^n, \quad t \geq 0, \quad (3)$$

where $(\cdot)_n$ is the Pochhammer symbol, while m , b_0 and Ω are the parameters of the SR fading.

With the system model above, the received SNR for a link is given by

$$\text{SNR}_{\text{up}} = \frac{p_{(2)}^s}{N_u} = \frac{p_{(1)}^e G_{(1)}^e G_{(2)}^s \lambda_u^2 W_t^2}{(4\pi d_{\text{up}})^2 L_{(1)}^e L_{(2)}^s L_{\text{add}} N_u}, \quad (4)$$

where N_u is the noise power of uplink. N_u can be calculated by $N_u = kBT_u$, where k is the Boltzmann's constant, B is the bandwidth of transmission and T_u denotes the total network noise temperature of the uplink.

The received SNR for a link is given by

$$\text{SNR}_{\text{down}} = \frac{p_{(2)}^e}{N_d} = \frac{p_{(1)}^s G_{(1)}^s G_{(2)}^e \lambda_d^2 W_t^2}{(4\pi d_{\text{down}})^2 L_{(1)}^s L_{(2)}^e L_{\text{add}} N_d}, \quad (5)$$

where N_d is the noise power of downlink and $p_{(2)}^e$ can be calculated as the same as $p_{(2)}^s$ with downlink parameters.

III. TIME DELAY ANALYSIS

A. Distance Distribution

In order to contribute expressions for average time delay in the following sections, we first need to characterize some basic distance distributions that stem from the stochastic geometry of the considered system. According to the relay selection strategy mentioned above, the downlink distance d_{down} is independent from θ_2 .

Since the correspondence between the central angle (the angle of the line from two points to the center of the Earth [15]) and distance is bijective, the distance distribution can be calculated via calculating the distribution of the central angle (the angle of the line between two points and the center of the Earth).

To facilitate the calculation of the uplink distance distribution, we use the CDF of the central angle. The central angle of the receiver and the relay satellite is denoted as θ_1 , and the central angle of the transmitter and the relay satellite is denoted as θ_2 .

Lemma 1: The PDF of the θ_1 from any specific one of the satellites in the constellation to the receiver is given by

$$f_{\theta_1}(\theta) = \frac{N_s \sin \theta}{2} \left(\frac{1 + \cos \theta}{2} \right)^{N_s - 1}, \quad 0 \leq \theta \leq \pi. \quad (6)$$

Proof 1: See Appendix A.

Lemma 2: The downlink distance distribution d_{up} is given by

$$F_{d_{\text{down}}}(d_0) = \begin{cases} 0, & d_0 \leq R_s - R_e \\ 1 - \left(1 - \left(\frac{d_0^2 - (R_s - R_e)^2}{4R_e R_s} \right) \right)^{N_s}, & \text{otherwise} \\ 1, & d_0 \geq R_s + R_e \end{cases} \quad (7)$$

Proof 2: See Appendix B.

Due to the relay selection strategy, θ_1 is an independent variable while θ_2 is a random variable associated with θ_1 .

It is important to note that we consider the probability of a satellite appearing in a circle ring with a fixed central angle θ_1 to be uniformly distributed. However, the probability of a satellite appearing in a circle ring with a fixed central angle θ_2 is weighted by $f_{\theta_1}(\theta)$.

Lemma 3: Given that the maximum central angle of the transmitter's spherical cap is β , the approximate CDF of $F_{\theta_2}(\beta)$ is given by

$$F_{\theta_2}(\beta) = \int_0^{2\pi} \int_0^\beta \frac{f_{\theta_1}(\psi(\theta, \phi))}{2\pi R_s^2 \sin \psi(\theta, \phi)} R_s^2 \sin \theta d\theta d\phi, \quad (8)$$

where $\psi(\theta, \phi)$ is represented by

$$\psi(\theta, \phi) = 2 \arccos \frac{R_s^2 + R_e^2 - \mathcal{D}^2(\theta, \phi, \Theta, 0)}{2R_s R_e}, \quad (9)$$

and Φ is the central angle between the transmitter and receiver. $\mathcal{D}^2(\theta_1, \phi_1, \theta_2, \phi_2)$ is an operator and can be expressed by

$$\begin{aligned} \mathcal{D}^2(\theta_1, \phi_1, \theta_2, \phi_2) &= R_e^2 + R_s^2 \\ &- 2R_e R_s (1 - (\cos \phi_1 \cos \phi_2 \cos(\theta_1 - \theta_2) + \sin \theta_1 \sin \theta_2)). \end{aligned} \quad (10)$$

Proof 3: See Appendix C.

Above all, we can obtain the uplink distance distribution d_{up} in the following lemma.

Lemma 4: The uplink distance distribution d_{up} is given by

$$F_{d_{\text{up}}}(d_0) = \begin{cases} 0, d_0 \leq R_s - R_e \\ \frac{d_0}{R_s R_s \sqrt{1 - \left(\frac{R_s^2 + R_e^2 - d_0^2}{2(R_s + R_e)} \right)^2}} \\ \times F_{\theta_2} \left(\arccos \left(\frac{R_s^2 + R_e^2 - d_0^2}{2(R_s + R_e)} \right) \right), \text{ else} \\ 1, d_0 \geq R_s + R_e \end{cases} \quad (11)$$

Proof 4: Since the expressions for the central angle θ_2 and downlink distance d_{up} is given by

$$\begin{aligned} d_{\text{up}} &= \sqrt{R_s^2 + R_e^2 - 2R_s R_e \cos \theta_2} \\ \theta_2 &= \arccos \left(\frac{R_s^2 + R_e^2 - d_{\text{up}}^2}{2R_s R_e} \right), \end{aligned} \quad (12)$$

and the uplink distance distribution d_{up} is given by (11).

B. Time Delay

We define the transmission time delay of a link as

$$\tau_Q = \frac{M}{B \log_2(1 + \text{SNR}_Q)}, Q \in \{\text{up}, \text{down}\}, \quad (13)$$

where M and B respectively denote the size of the packet and the bandwidth of transmission. Thus we can derive the total time delay τ_{total} in following theorem.

Theorem 1: The average time delay of downlink $\bar{\tau}_{\text{down}}$ is given by

$$\bar{\tau}_{\text{down}} = \frac{M}{B \log_2 \left(1 + \frac{p_{(1)}^s G_{(1)}^s G_{(2)}^e \lambda_d^2 (\Omega + 2b_0)}{(4\pi d_{\text{down}})^2 L_{(1)}^s L_{(2)}^e L_{\text{add}} N_d} \right)}. \quad (14)$$

Proof 5: See Appendix D.

Theorem 2: The average time delay of uplink $\bar{\tau}_{\text{up}}$ is given by

$$\bar{\tau}_{\text{up}} = \int_0^\infty \frac{M}{B \log_2(1 + \gamma)} f_{\text{SNR}_{\text{up}}}(\gamma) d\gamma, \quad (15)$$

where

$$\begin{aligned} f_{\text{SNR}_{\text{up}}}(\gamma) &= \int_{(R_s - R_e)^2}^{(R_s + R_e)^2} \frac{\sqrt{u}}{2} \left(\frac{2b_0 m}{2b_0 m + \Omega} \right)^m \exp \left(-\frac{z(\gamma)u}{2b_0} \right) \\ &\times \frac{1}{2b_0} \sum_{n=0}^\infty \frac{(m)_n}{(1)_n n!} \left(\frac{\Omega z(\gamma)u}{2b_0(2b_0 m + \Omega)} \right)^n f_{d_{\text{up}}}(\sqrt{u}) du, \end{aligned} \quad (16)$$

and $z(\gamma) = \frac{(4\pi)^2 L_{(1)}^e L_{(2)}^s L_{\text{add}} N_u \gamma}{p_{(1)}^e G_{(1)}^e G_{(2)}^s \lambda_u^2}$.

Proof 6: See Appendix E.

C. Optimality Analysis

Due to the relay selection strategy and earth blockage, the transmitter and receiver can only communicate with satellites within a maximum distance L_{max} :

$$L_{\text{max}} = 2R_e \sin \left(\frac{1}{2} \arccos \left(\frac{R_e}{R_s} \right) \right). \quad (17)$$

Under the premise of satisfying the above inequalities, we solve the optimization problem below and explore the optimal relay position of the satellite through numerical results.

$$\theta^* = \underset{0 \leq \theta \leq \Theta}{\text{argmin}} \bar{\tau}_{\text{up}} + \bar{\tau}_{\text{down}}. \quad (18)$$

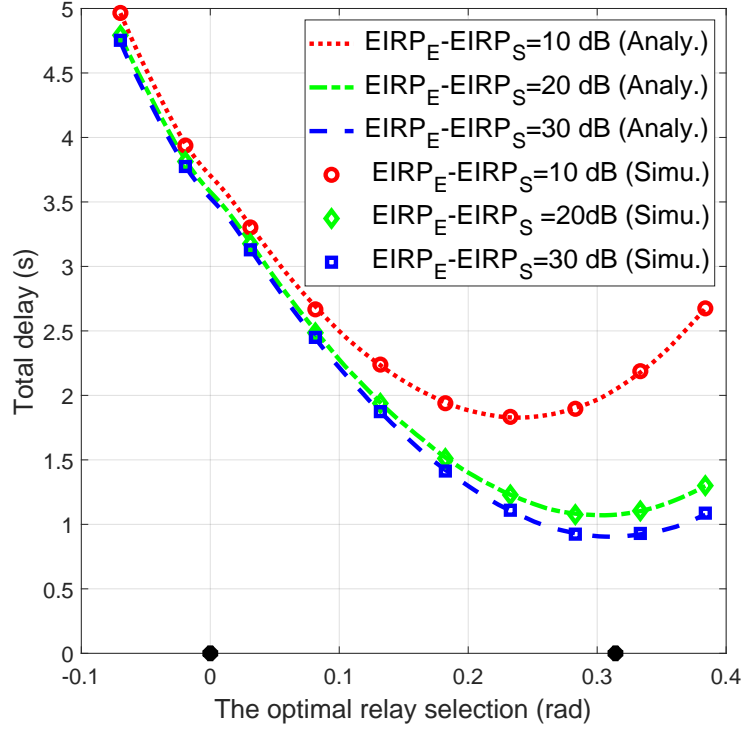


Fig. 2: Total time delay with different relay selection.

In Fig.2, we use markers to denote the polar angle coordinate position of the terrestrial station. The horizontal coordinate is the polar angle of the ideal relay satellite. In the Monte-Carlo simulation, we search for the closest satellite to the ideal satellite coordinates as a relay satellite to calculate the uplink and downlink time delays. It can be seen that choosing the closest satellite to the receiver is a good suboptimal strategy when the ratio of uplink and downlink power differs significantly.

IV. NUMERICAL RESULTS

In this section, we verify the accuracy of the derived expressions using Monte-Carlo simulations. In addition, we study the influence of various system parameters on the performance of the considered system. In all the figures, markers represent the derived analytical results while the solid lines represent the Monte-Carlo simulations. The system parameters used in the simulations are summarized in Table I.

In Fig.3, we plot total delay for different fixed number of satellites and study the effect of increasing the altitude of satellite. The results show that transmission delay increase as the the

TABLE I: Table of Notations.

<i>Notations</i>	<i>Description</i>	<i>Value(Default)</i>
N_s	Number of satellites	500
$R_e; R_s$	Radius of the Earth; satellites	6371; 6871 (km)
$N_u; N_d$	Noise power of uplink; downlink	3.6×10^{-12} ; 3.6×10^{-12}
$B_u; B_d$	Bandwidth of uplink; downlink	0.5; 0.25 (GHz)
$p_{(1)}^s G_{(1)}^s; p_{(1)}^e G_{(1)}^e$	Effective isotropic radiated power at relay satellite; transmitter	30; 60 (dB)
L_{add}	Link additional loss	3 (dB)
$\lambda_d; \lambda_u$	Carrier wavelength of downlink; uplink	0.0231; 0.015 (m)
$\Omega; b_0; m$	Line-of-sight component; scatter component; Nakagami parameter	1.29; 0.158; 19.4
M	The size of the packet	0.5 Gbit

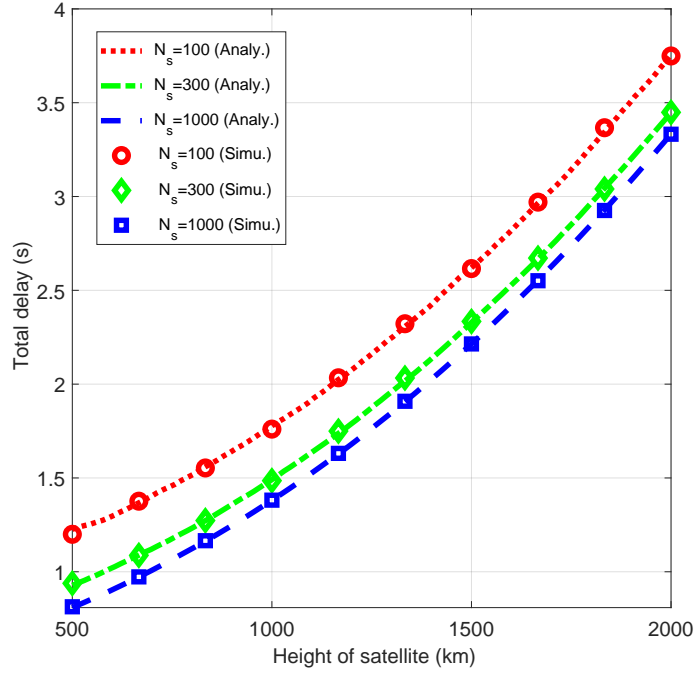


Fig. 3: Total time delay with different number of satellite.

height of satellite and we can observe that for a fixed altitude time delay reduces as we increase the number of satellite.

In Fig.4, the time delay is studied under different values for the distance between the transmitter and receiver for companies OneWeb, Telesat and SpaceX with altitudes $h = 1200$ km, $h = 1150$

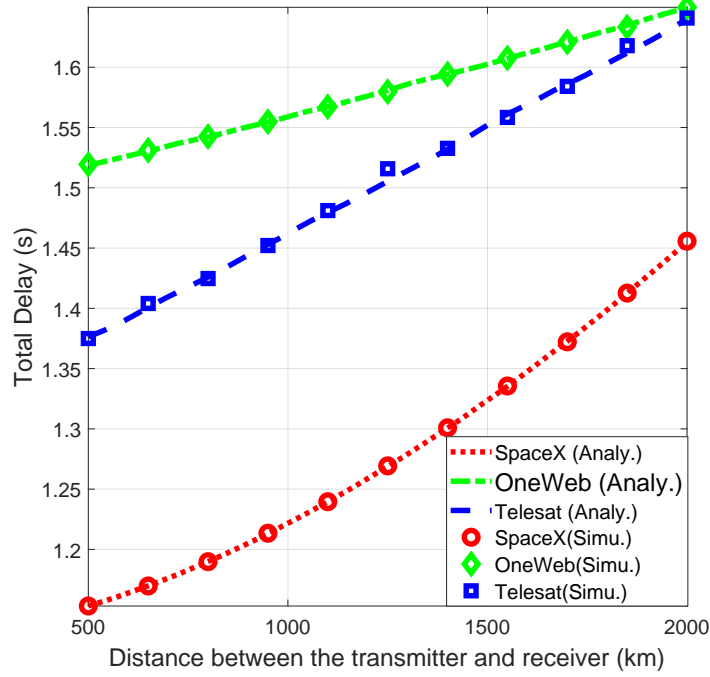


Fig. 4: Total time delay with different distance between the transmitter and receiver.

km and $h = 1110$ km [16]. Other parameters such as the number of satellites, effective isotropic radiated power, carrier frequency, bandwidth, etc. are referenced in [16].

Fig.5 illustrates the scenario of a long distance transmission containing multiple hops. We set the total transmission distance to 15000 km and calculate the minimum number of hops required at different altitude satellites according to (17). As the altitude of the satellite increases, it is less affected by ground obscuration and the maximum distance between both sides of communication on the ground is increasing.

V. CONCLUSION

In this work, we propose a suboptimal satellite relay selection strategy in terrestrial-satellite-terrestrial scenario. Though deriving theoretical expressions of the downlink and uplink distance distribution, we give a expression of total transmission delay. We have verified all the derived expressions using Monte-Carlo simulations and ensured perfect fit. In simulation, we explore the conditions for the proposed strategy to reach optimal and provide the numerical results about

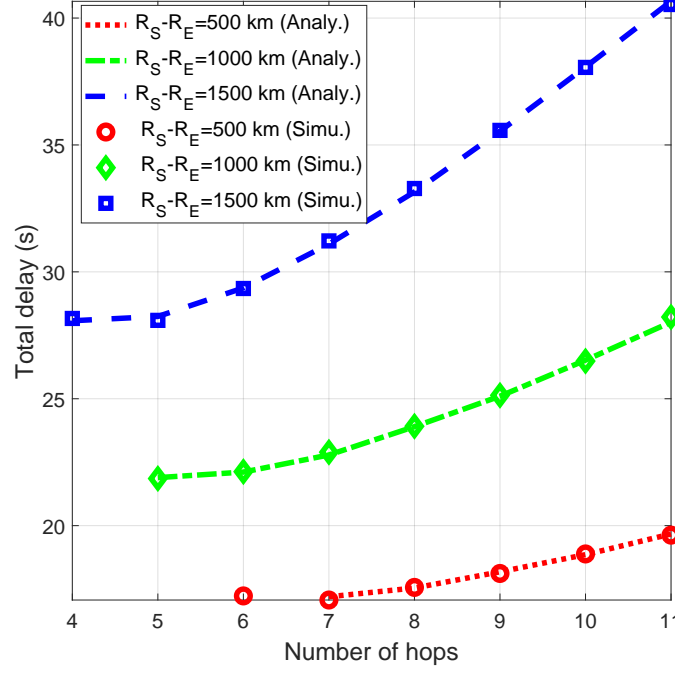


Fig. 5: Total time delay with different hops in fixed long-distance transmission.

the influence of the altitudes of the satellites, their numbers, the distance between two terrestrial stations on the performance of the delay.

VI. ACKNOWLEDGEMENT

This work was supported by the National Key Research and Development Program of China (No. 2021YFB2900404).

APPENDIX A

PROOF OF LEMMA 1

For a homogeneous BPP, the probability of the satellite locates in a spherical cap with central angle θ is equal to the ratio of the area of θ to the total surface area of the sphere. So, we can obtain

$$\begin{aligned}
 \mathbb{P}[\theta_1 \leq \theta] &= \frac{\int_0^{2\pi} \int_0^\theta R_s \sin(\theta_1) d\theta_1 d\phi}{4\pi R_s^2} \\
 &= \frac{2\pi R_s^2 (1 - \cos \theta)}{4\pi R_s^2}, 0 \leq \theta \leq \pi.
 \end{aligned} \tag{19}$$

Due to the channel assignment by which the serving satellite is the nearest one among all the N_s i.i.d. satellites, the CDF of the θ_1 from any specific one of the satellites in the constellation to the receiver is given by

$$\begin{aligned} F_{\theta_1}(\theta) &= 1 - \prod_{i=1}^{N_s} \mathbb{P}[\theta_1 \geq \theta] \\ &= 1 - \left(1 - \frac{2\pi R_s^2(1 - \cos \theta)}{4\pi R_s^2}\right)^{N_s} \\ &= 1 - \left(\frac{1 + \cos \theta}{2}\right)^{N_s}, \end{aligned} \quad (20)$$

The PDF of θ_1 is

$$f_{\theta_1}(\theta) = \frac{d}{d\theta} F_{\theta_1}(\theta) = \frac{N_s \sin \theta}{2} \left(\frac{1 + \cos \theta}{2}\right)^{N_s-1}, \quad (21)$$

where $\frac{d}{d\theta}$ means take the derivative with respect to θ .

APPENDIX B

PROOF OF LEMMA 2

In the authors' work [7], the PDF of d_{down} was derived as shown in the below lemma.

Due to the channel assignment by which the serving satellite is the nearest one among all the N_s i.i.d. satellites, the PDF of the d_{down} from any specific one of the satellites in the constellation to the user is given by

$$f_{d_{\text{down}}}(d_0) = N_s \left(1 - \frac{d_0^2 - (R_s - R_e)^2}{4R_e R_s}\right)^{N_s-1} \frac{d_0}{2R_e R_s}, \quad (22)$$

for $R_s - R_e \leq d_0 \leq R_s + R_e$ while $f_{d_{\text{down}}}(d_0) = 0$ otherwise. The CDF can be expressed as

$$F_{d_{\text{down}}}(d_0) = \begin{cases} 0, & d_0 \leq R_s - R_e \\ 1 - \left(1 - \left(\frac{d_0^2 - (R_s - R_e)^2}{4R_e R_s}\right)\right)^{N_s}, & \text{else} \\ 1, & d_0 \geq R_s + R_e \end{cases} \quad (23)$$

APPENDIX C

PROOF OF LEMMA 3

To derive the distribution of θ_2 , the following steps are taken: (i): assuming that the coordinate position of the satellite is (R_s, θ_0, ϕ_0) ; (ii): in order to calculate the probability of the satellite appearing in the spherical cap (corresponds to the central angle β), perform a double integration

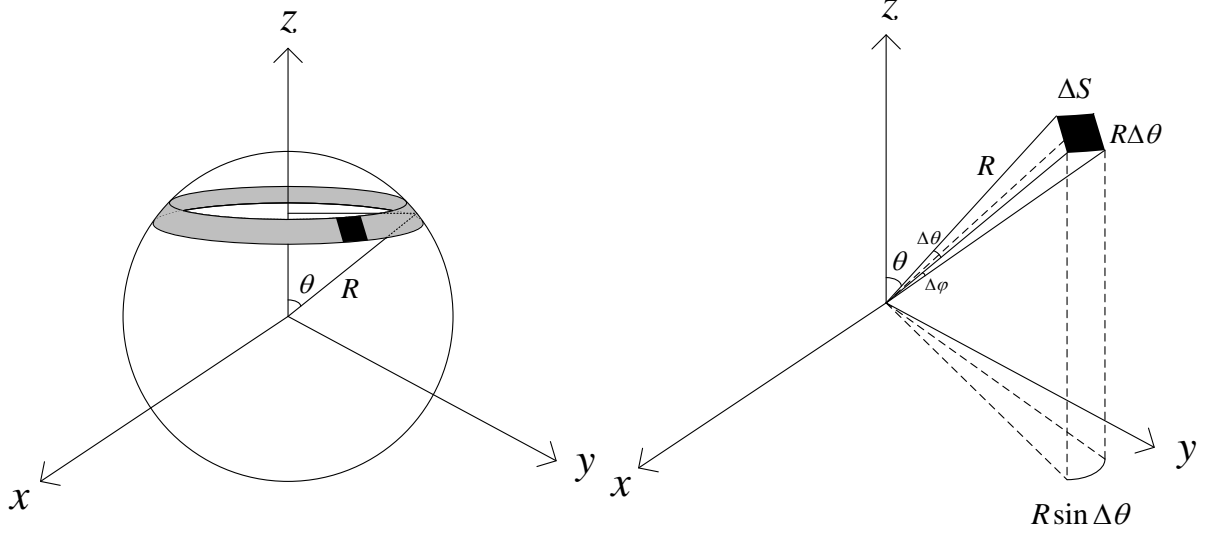


Fig. 6: Illustrations of Lemma 3 and Lemma 4.

over the probability of the satellite with respect to θ_0 and ϕ_0 , where $0 \leq \theta_0 \leq \beta$ and $0 \leq \phi_0 \leq 2\pi$;
 (iii): the probability of occurrence at (R_s, θ_0, ϕ_0) is weighted by $\frac{f_{\theta_1}(\psi(\theta, \phi))}{2\pi R_s^2 \sin \psi(\theta, \phi)}$.

Given that the maximum central angle of the transmitter's spherical cap is 2β , the approximate CDF of $F_{\theta_2}(\beta)$ is given by

$$F_{\theta_2}(\beta) = \int_0^{2\pi} \int_0^\beta \frac{f_{\theta_1}(\psi(\theta, \phi))}{2\pi R_s^2 \sin \psi(\theta, \phi)} R_s^2 \sin \theta d\theta d\phi. \quad (24)$$

And $\psi(\theta, \phi)$ is represented by

$$\psi(\theta, \phi) = 2 \arccos(\sin \theta \sin \Theta \cos \phi + \cos \theta \cos \Theta), \quad (25)$$

where Θ is the central angle between the transmitter and receiver.

APPENDIX D

PROOF OF THEOREM 1

The average time delay of uplink $\bar{\tau}_{\text{down}}$ is given by

$$\bar{\tau}_{\text{down}} = \frac{M}{B \log_2(1 + \overline{\text{SNR}}_{\text{down}})}, \quad (26)$$

where $\mathbb{E}[\cdot]$ denotes taking the mathematical expectation.

The average central angle $\bar{\theta}_1$ is given by:

$$\begin{aligned}
\bar{\theta}_1 &= \mathbb{E}[\theta_1] = \int_0^\pi 1 - F_{\theta_1}(\theta) d\theta \\
&= \int_0^\pi \left(\frac{1 + \cos \theta}{2} \right)^{N_s} d\theta = \int_0^\pi \left(\cos \frac{\theta}{2} \right)^{2N_s} d\theta \\
&= 2 \int_0^{\frac{\pi}{2}} (\cos \theta)^{2N_s} d\theta = \pi \prod_{n=0}^{N_s-1} \frac{2N_s - 2n - 1}{2N_s - 2n}
\end{aligned} \tag{27}$$

The average distance of downlink \bar{d}_{down} can be calculated by:

$$\bar{d}_{\text{down}} = \sqrt{R_e^2 + R_s^2 - 2R_e R_s \cos \bar{\theta}_1}. \tag{28}$$

According to [14], the moment-generating function (MGF) of the instantaneous power can be shown to be

$$M_{W_t^2}(\sigma) = \frac{(2b_0 m)^m (1 + 2b_0 \sigma)^{m-1}}{[(2b_0 m + \Omega)(1 + 2b_0 \sigma) - \Omega]^m}, \sigma \geq 0. \tag{29}$$

The mathematical expectation of W_t^2 is given by:

$$\mathbb{E}[W_t^2] = \frac{d}{d\sigma} M_{W_t^2}(0) = \Omega + 2b_0. \tag{30}$$

Recall (5), by substituting (27), (28) and (30) into (26), we obtain the average time delay of downlink $\bar{\tau}_{\text{down}}$:

$$\bar{\tau}_{\text{down}} = \frac{M}{B \log_2 \left(1 + \frac{p_{(1)}^s G_{(1)}^s G_{(2)}^e \lambda_d^2 (\Omega + 2b_0)}{(4\pi \bar{d}_{\text{down}})^2 L_{(1)}^s L_{(2)}^e L_{\text{add}} N_d} \right)}. \tag{31}$$

APPENDIX E

PROOF OF THEOREM 2

Recall (4), since W_t^2 and d_{down} are independent random variables, the PDF of SNR_{up} is a two-dimensional random variable and can be given by

$$\begin{aligned}
 f_{\text{SNR}_{\text{up}}}(\gamma) &= \mathbb{P} \left(\frac{p_{(1)}^e G_{(1)}^e G_{(2)}^s \lambda_u^2 W_t^2}{(4\pi d_{\text{up}})^2 L_{(1)}^e L_{(2)}^s L_{\text{add}} N_u} = \gamma \right) \\
 &= \int_{(R_s - R_e)^2}^{(R_s + R_e)^2} u f_{W_t^2}(z(\gamma)u) f_{d_{\text{down}}^2}(u) du \\
 &= \int_{(R_s - R_e)^2}^{(R_s + R_e)^2} \frac{\sqrt{u}}{2} f_{W_t^2}(z(\gamma)u) f_{d_{\text{down}}}(\sqrt{u}) du \\
 &= \int_{(R_s - R_e)^2}^{(R_s + R_e)^2} \frac{\sqrt{u}}{2} \left(\frac{2b_0 m}{2b_0 m + \Omega} \right)^m \frac{1}{2b_0} \exp \left(-\frac{z(\gamma)u}{2b_0} \right) \\
 &\quad \times \sum_{n=0}^{\infty} \frac{(m)_n}{(1)_n n!} \left(\frac{\Omega z(\gamma)u}{2b_0(2b_0 m + \Omega)} \right)^n f_{d_{\text{up}}}(\sqrt{u}) du,
 \end{aligned} \tag{32}$$

where $z(\gamma) = \frac{(4\pi)^2 L_{(1)}^e L_{(2)}^s L_{\text{add}} N_u \gamma}{p_{(1)}^e G_{(1)}^e G_{(2)}^s \lambda_u^2}$.

The average time delay of uplink $\bar{\tau}_{\text{up}}$:

$$\begin{aligned}
 \bar{\tau}_{\text{up}} &= \mathbb{E} \left[\frac{M}{B \log_2(1 + \text{SNR}_{\text{up}})} \right] \\
 &= \int_0^{\infty} \frac{M}{B \log_2(1 + \gamma)} f_{\text{SNR}_{\text{up}}}(\gamma) d\gamma.
 \end{aligned} \tag{33}$$

REFERENCES

- [1] C. De Alwis, A. Kalla, Q.-V. Pham, P. Kumar, K. Dev, W.-J. Hwang, and M. Liyanage, "Survey on 6g frontiers: Trends, applications, requirements, technologies and future research," *IEEE Open Journal of the Communications Society*, vol. 2, pp. 836–886, 2021.
- [2] O. Kodheli, E. Lagunas, N. Maturo, S. K. Sharma, B. Shankar, J. F. M. Montoya, J. C. M. Duncan, D. Spano, S. Chatzinotas, S. Kisseleff *et al.*, "Satellite communications in the new space era: A survey and future challenges," *IEEE Communications Surveys & Tutorials*, vol. 23, no. 1, pp. 70–109, 2020.
- [3] M. Sheetz and M. Petrova, "Why in the next decade companies will launch thousands more satellites than in all of history," *CNBC. Last accessed October*, vol. 22, p. 2021, 2019.
- [4] Y. Ma, T. Lv, G. Pan, Y. Chen, and M.-S. Alouini, "On secure uplink transmission in hybrid rf-fso cooperative satellite-aerial-terrestrial networks," *IEEE Transactions on Communications*, vol. 70, no. 12, pp. 8244–8257, 2022.

- [5] R. Wang, M. A. Kishk, and M.-S. Alouini, "Ultra-dense LEO satellite-based communication systems: A novel modeling technique," *IEEE Communications Magazine*, vol. 60, no. 4, pp. 25–31, 2022.
- [6] Y. Tian, G. Pan, H. ElSawy, and M.-S. Alouini, "Satellite-aerial communications with multi-aircraft interference," *IEEE Transactions on Wireless Communications*, 2023, early access.
- [7] N. Okati, T. Riihonen, D. Korpi, I. Angervuori, and R. Wichman, "Downlink coverage and rate analysis of low earth orbit satellite constellations using stochastic geometry," *IEEE Transactions on Communications*, vol. 68, no. 8, pp. 5120–5134, 2020.
- [8] A. Talgat, M. A. Kishk, and M.-S. Alouini, "Stochastic geometry-based analysis of leo satellite communication systems," *IEEE Communications Letters*, vol. 25, no. 8, pp. 2458–2462, 2020.
- [9] R. Wang, A. Talgat, M. A. Kishk, and M.-S. Alouini, "Conditional contact angle distribution in leo satellite-relayed transmission," *IEEE Communications Letters*, vol. 26, no. 11, pp. 2735–2739, 2022.
- [10] R. Wang, M. A. Kishk, and M.-S. Alouini, "Reliability analysis of multi-hop routing in multi-tier leo satellite networks," *IEEE Transactions on Wireless Communications*, 2023, early access.
- [11] K. Belbase, Z. Zhang, H. Jiang, and C. Tellambura, "Coverage analysis of millimeter wave decode-and-forward networks with best relay selection," *IEEE Access*, vol. 6, pp. 22 670–22 683, 2018.
- [12] R. Wang, M. A. Kishk, and M.-S. Alouini, "Evaluating the accuracy of stochastic geometry based models for LEO satellite networks analysis," *IEEE Communications Letters*, vol. 26, no. 10, pp. 2440–2444, 2022.
- [13] Z. Lou, B. E. Y. Belmekki, and M.-S. Alouini, "Coverage analysis of hybrid RF/THz networks with best relay selection," *IEEE Communications Letters*, 2023.
- [14] A. Abdi, W. Lau, M.-S. Alouini, and M. Kaveh, "A new simple model for land mobile satellite channels: first- and second-order statistics," *IEEE Transactions on Wireless Communications*, vol. 2, no. 3, pp. 519–528, 2003.
- [15] R. Wang, M. A. Kishk, and M.-S. Alouini, "Stochastic geometry-based low latency routing in massive LEO satellite networks," *IEEE Transactions on Aerospace and Electronic Systems*, vol. 58, no. 5, pp. 3881–3894, 2022.
- [16] I. Del Portillo, B. G. Cameron, and E. F. Crawley, "A technical comparison of three low earth orbit satellite constellation systems to provide global broadband," *Acta astronautica*, vol. 159, pp. 123–135, 2019.